

# Passivity of Time-Delayed Whole-Body Operational Space Control with Series Elastic Actuation

Ye Zhao and Luis Sentis\*

**Abstract**—Whole-Body Control has been extensively used to achieve humanoid robot force and motion tasks simultaneously during recent years. However, most existing results have not incorporated low-level actuator dynamics and time delays yet. In this study, we propose a novel time-delayed Whole-Body Operational Space control (WBOSC) with series elastic actuator (SEA) dynamics. This type of controller generalizes our previously proposed distributed control structure to multi-input and multi-output free floating humanoid robotic systems. Namely, Cartesian stiffness control is adopted to design the WBOSC at the centralized level while motor damping control is implemented at the embedded level to remedy the stability deterioration caused by time delays. Additionally, embedded-level torque feedback control is formulated and physically interpreted as a shaping of the motor inertia. To ensure passivity, we separate the overall system into two subsystems interconnected in a feedback configuration. By the Lyapunov-Krasovskii functional technique, we propose a delay-dependent passivity criterion of the closed-loop system in the form of linear matrix inequalities (LMIs), and solve for the allowable maximum time delays via the passivity criterion. Numerical simulations of a dynamic locomotion process are used to validate the proposed passivity criterion and the WBOSC framework.

## I. INTRODUCTION

Whole-Body Control (WBC) has spawned a vast number of theoretical and implementation results to enable torque-controlled humanoid robots to perform complex full-body control tasks during the past few decades. The majority of WBC methods fall into two categories: null-space projection-based methods [1], [2], [3], [4], [5], [6], [7], and optimization-based methods [8], [9], [10], [11], [12], [13]. Recently, increasing attention has been placed on hardware implementations such as Whole-Body Operational Space Control (WBOSC) on a point-feet bipedal robot for dynamic balancing [14] and centroidal-momentum-based whole-body controllers [10], [15], [12]. However, real hardware performance frequently falls far short of the expectations, especially due to numerous practical issues arising from delayed communication and sensing processes [16], [17], actuator dynamics [10], [18], [19] and unmodelled mechanical compliance [14]. These issues motivate this work which attempts to reduce the performance gap between theoretical foundations and real implementations. In particular, our focus is to explicitly incorporate time delays and series elastic actuator (SEA) dynamics into the WBOSC formalism and reason about the conditions under which the closed-loop stability and passivity are preserved.

As a robustness property, passivity is an essential requirement to ensure the coupled stability of robotic systems interacting with unknown dynamic environments [20]. The pioneering work in [21] proposed a necessary and sufficient condition for the passivity of sampled-data systems when designing haptic interfaces. However, the proposed passivity criterion is conservative in that the haptic display may remain stable even if violating the passivity condition (i.e., become “active”). Additionally, time delays are ignored in this work. Along the same line of research, the authors in [22] derived passivity and stability boundary conditions with time delays. Comparisons between passivity and stability are extensively investigated by analyzing the influence of various system parameters including sampling rate, time delay, physical damping and the mass. However, all the results above are restricted to single degree-of-freedom (DOF) systems, which severely limit their applicability to high-DOF humanoid robots.

In Albu-Schäffer and Ott’s seminal work on multi-DOF Cartesian impedance control with flexible joint dynamics [19], [23], joint torque feedback was physically interpreted as a scaling of the motor inertia such that the passivity of the closed-loop system is ensured. Nevertheless, these works are limited to manipulations. Applying passivity-based impedance controllers to full-body humanoid control was first proposed in [24]. This type of compliant controller designed gravity compensation and adaptation to unknown external forces. The desired ground reaction forces were distributed among a set of predefined contact points and directly mapped to the joint torque. Recently, the authors in [25] proposed a compliant multi-contact balancing controller while guaranteeing the overall system passivity. However, the involved tasks are not strictly hierarchical, and prioritized multi-task control based on null-space projection methods are still open to be explored to date. All the above works are limited in that none of them modeled or investigated the effect of time delays, as it is done in this study.

Stability under time delay [26] has been extensively studied in the teleoperation community [27], [28]. To overcome the instability caused by time delays, a conservative passivity based method [29] was proposed to guarantee stable teleoperation performance. The authors employed Lyapunov-Krasovskii functionals to enforce energetic passivity of closed-loop nonlinear teleoperators by passifying the combination of the delayed communication and control blocks altogether. The delays are allowed to be unknown but have to be finite constant, which is a conservative assumption for the real hardware. In previous work [30] closely

\*The authors are with the Department of Mechanical Engineering at The University of Texas at Austin, USA 78712 (emails: yezhao@utexas.edu, lsentis@austin.utexas.edu)

related to this paper, asymmetric and time-varying delays were handled by proposing stability criteria of networked teleoperation systems via linear matrix inequality (LMI) techniques. However, their derived LMIs are time-invariant (i.e., no time-varying matrices involved). Recently, a few methods were proposed that dealt with time-varying LMIs by solving them online in [31] and by convexifying matrices as a polytope of parametric matrices [32]. In this study, the proposed LMI-based passivity criterion involves both time-varying delays and time-varying system matrices, and we solve it numerically.

Series elastic actuators (SEAs) [18], [33], as an emerging actuation mechanism, provide considerable advantages in compliant and safe environmental interaction and force sensing. Cascaded impedance control architectures have been increasingly adopted for SEA systems over the past few years [18], [34], [35]. This type of architecture nests feedback control loops, i.e., an inner-torque loop and an outer-impedance loop for the task-level control. The authors of [34] proposed to embed a motor velocity loop inside the torque feedback loop. This velocity feedback allows the use of integral gains to counteract static errors such as drivetrain friction while maintaining the system passivity. Once more, the above works either do not systematically analyze the effect of time delays or at most, model mild time delays which are not applicable to real systems with the large time delays inherent in serial communication channels.

A class of distributed control architectures for latency-prone robotic systems was proposed in our previous work [16]. A central phenomenon has been observed experimentally that the stability of high impedance distributed controllers is highly sensitive to damping time delay but much less to stiffness time delay. Therefore, we suggest a distributed controller where damping feedback effort is executed in proximity to the control plant, and stiffness feedback effort is implemented in a latency-prone centralized control process. Recently, we extended this distributed strategy to the SEA cascaded control structure with inner-torque and outer-impedance feedback loops [35]. This paradigm motivates us to design a WBOSC with Cartesian position feedback at the centralized level and motor damping feedback at the embedded level. Note that, our prior works mainly focus on SISO systems instead of the MIMO ones, which will be the focus of this study.

In light of the discussions above, the rest of this paper is outlined as follows. We first propose a theoretical formalism of the WBOSC architecture with embedded-level SEA dynamics in Section II. Section III formulates a centralized-level WBOSC control with time delays. A passivity criterion is proposed by using Lyapunov-Krasovskii functionals in Section IV. Simulation results are shown in Section V. The final section discusses future works. The proposed passivity has two inherent merits: (i) increase the robustness of the whole system, and (ii) provide advantages in the compositional analysis of large-scale and complex control systems, such as the WBOSC coupled with SEA controllers examined in this study. As far as the authors' knowledge, this is the first

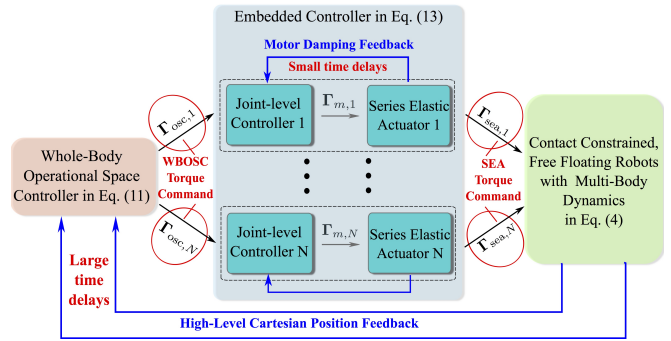


Fig. 1. Time-delayed Whole-Body Operational Space Control architecture.

attempt to design time-delayed WBOSC with SEA dynamics while guaranteeing the system passivity.

## II. WHOLE-BODY OPERATIONAL SPACE CONTROL FORMALISM

Lagrange rigid multi-body dynamics are ubiquitously used in the robotics community [36], [37]. However, low-level actuator dynamics and time delays are largely overlooked but indeed pose a considerable threat to the closed-loop system stability and performance. In this study, we propose a Whole-Body Operational Space Control (WBOSC) formalism incorporating embedded-level SEA dynamics in Section II and distributed delays in Section III. An overall control diagram is shown in Fig. 1.

### A. WBOSC with SEA Dynamics

Actuator dynamics are frequently ignored in the multi-body dynamics analysis due to its intrinsic complexity. The authors in [19], [38], [39] emphasized the importance of actuator dynamics in conventional rigid multi-body control and therefore, incorporated them into the whole-body controller formalism. Even so, extending the actuator-aware whole-body controller to free floating base dynamics with supporting contact constraints [2] has not been explored yet. This motivates our study in this paper. First, let us impose a few necessary assumptions.

*Assumption 1:* The motor rotation axis coincides with the principal axis of inertia. Thus the rotor inertia has a uniform distribution around its rotational axis [40].

*Assumption 2:* The rotor kinetic energy is dominated by pure rotation with respect to an inertial frame [39].

To derive the equations of motion, we define kinetic and potential energies based on rigid multi-body dynamics and elastic actuator dynamics. Given Assumption 1, the kinetic energy is represented as

$$\mathcal{T} = \frac{1}{2} \dot{\mathbf{q}}^T \mathbf{A}(\mathbf{q}) \dot{\mathbf{q}} + \dot{\mathbf{q}}^T \mathbf{C}(\mathbf{q}) \dot{\boldsymbol{\theta}} + \frac{1}{2} \dot{\boldsymbol{\theta}}^T \mathbf{B} \dot{\boldsymbol{\theta}}, \quad (1)$$

where  $\mathbf{q} = (\mathbf{q}_b, \mathbf{q}_j)^T \in \mathbb{R}^{6+n}$  includes a free floating base state vector  $\mathbf{q}_b \in \mathbb{R}^6$  composed of three prismatic joints and three rotational joints, and an actuated joint angle state vector  $\mathbf{q}_j \in \mathbb{R}^n$ ;  $\boldsymbol{\theta} \in \mathbb{R}^n$  corresponds to the motor angle state vector;  $\mathbf{A}(\mathbf{q}) \succ \mathbf{0}$  is the inertia matrix of the multi-body dynamics;  $\mathbf{C}(\mathbf{q})$  represents the coupled inertia between

motor-side and joint-side dynamics;  $\mathbf{B}$  is a constant diagonal matrix that denotes the rotor inertia after the gear ratio square scaling. By Assumption 2, the rotor inertia is the one along its principal axis of rotation,  $z$ -axis, represented by  $I_{zz_i}$ .

The potential energy has two components: gravitational energy  $\mathcal{P}_g(\mathbf{q})$  and elastic potential energy  $\mathcal{P}_e(\mathbf{q}, \boldsymbol{\theta})$ .

$$\mathcal{P} = \mathcal{P}_g(\mathbf{q}) + \mathcal{P}_e(\mathbf{q}, \boldsymbol{\theta}). \quad (2)$$

By the Lagrangian  $\mathcal{L} = \mathcal{T} - \mathcal{P}$  and Euler-Lagrangian derivations [41], we have

$$\begin{aligned} & \begin{pmatrix} \mathbf{A}(\mathbf{q}) & \mathbf{C}(\mathbf{q}) \\ \mathbf{C}^T(\mathbf{q}) & \mathbf{B} \end{pmatrix} \begin{pmatrix} \ddot{\mathbf{q}} \\ \ddot{\boldsymbol{\theta}} \end{pmatrix} + \begin{pmatrix} \mathbf{b} & \mathbf{b}_q \\ \mathbf{b}_\theta^T & \mathbf{0} \end{pmatrix} \begin{pmatrix} \dot{\mathbf{q}} \\ \dot{\boldsymbol{\theta}} \end{pmatrix} \\ & + \begin{pmatrix} \mathbf{g}(\mathbf{q}) \\ \mathbf{0} \end{pmatrix} + \begin{pmatrix} \mathbf{J}_s^T \mathbf{F}_r \\ \mathbf{0} \end{pmatrix} = \begin{pmatrix} \mathbf{U}^T \boldsymbol{\Gamma}_{\text{sea}} \\ -\boldsymbol{\Gamma}_{\text{sea}} \end{pmatrix} + \begin{pmatrix} \mathbf{0} \\ \boldsymbol{\Gamma}_m \end{pmatrix}, \quad (3) \end{aligned}$$

where  $\mathbf{b} = \mathbf{b}(\mathbf{q}, \dot{\mathbf{q}}, \dot{\boldsymbol{\theta}})$  denotes the Coriolis and centrifugal forces;  $\mathbf{b}_q = \mathbf{b}_q(\mathbf{q}, \dot{\mathbf{q}})$  and  $\mathbf{b}_\theta = \mathbf{b}_\theta(\mathbf{q}, \dot{\boldsymbol{\theta}})$  are derived from the Lagrange formalism in [38];  $\mathbf{g}(\mathbf{q})$  denotes the gravitational forces;  $\mathbf{U}$  is a selection matrix that chooses actuated joint states;  $\boldsymbol{\Gamma}_{\text{sea}} = \mathbf{K}(\boldsymbol{\theta} - \mathbf{q}_j)$  denotes the sensed SEA torque from spring deflection, where the diagonal matrix  $\mathbf{K}$  represents the joint spring stiffness;  $\boldsymbol{\Gamma}_m$  represents the motor torque. The first block row in Eq. (3) represents the joint-side dynamics while the second block row represents the motor-side dynamics. A distinct feature of this formalism is its incorporation of the contact Jacobian force and free floating dynamics [42], which characterize the features of under-actuated humanoid locomotion dynamics.

*Assumption 3:* To make the multi-body dynamics tractable, we ignore the inertia coupling between joint-side and motor-side dynamics [19], [38]. That is,  $\mathbf{C}(\mathbf{q}) \approx \mathbf{0}$ ,  $\mathbf{b} \approx \mathbf{b}(\mathbf{q}, \dot{\mathbf{q}})$ ,  $\mathbf{b}_q \approx \mathbf{0}$ ,  $\mathbf{b}_\theta \approx \mathbf{0}$ .

Essentially, the assumption above is built upon the approximation that the rotational kinetic energy of the motor-gearbox assembly is dominated by its self-rotation [39]. Based on Assumption 3, Eq. (3) is simplified to

$$\mathbf{A}(\mathbf{q})\ddot{\mathbf{q}} + \mathbf{N}(\mathbf{q}, \dot{\mathbf{q}}) + \mathbf{J}_s^T \mathbf{F}_r = \mathbf{U}^T \boldsymbol{\Gamma}_{\text{sea}}, \quad (4)$$

$$\mathbf{B}\ddot{\boldsymbol{\theta}} + \boldsymbol{\Gamma}_{\text{sea}} = \boldsymbol{\Gamma}_m, \quad (5)$$

$$\boldsymbol{\Gamma}_{\text{sea}} = \mathbf{K}(\boldsymbol{\theta} - \mathbf{q}_j), \quad (6)$$

where  $\mathbf{N}(\mathbf{q}, \dot{\mathbf{q}}) = \mathbf{b}(\mathbf{q}, \dot{\mathbf{q}})\dot{\mathbf{q}} + \mathbf{g}(\mathbf{q})$ ; Later on, we will design a WBOSC controller computing the desired joint torque command  $\boldsymbol{\Gamma}_{\text{osc}}$ , which is sent as control inputs to the embedded-level SEAs.

### B. Embedded-Level SEA Controller

The embedded-level SEA controller comprises both torque and motor damping feedback loops (for instance, the control architecture in [34]). By torque feedback control, the control command  $\boldsymbol{\Gamma}_{\text{osc}}$  sent to the embedded-level controller and the SEA torque  $\boldsymbol{\Gamma}_{\text{sea}}$  actuating the robot joint are related by

$$\begin{aligned} \boldsymbol{\Gamma}_m &= \mathbf{B}\mathbf{B}_s^{-1}\boldsymbol{\Gamma}_{\text{osc}} + (\mathbf{I} - \mathbf{B}\mathbf{B}_s^{-1})\boldsymbol{\Gamma}_{\text{sea}} - \mathbf{B}\mathbf{B}_s^{-1} \cdot \mathbf{D}_\theta \dot{\boldsymbol{\theta}} \\ &= \mathbf{B}\mathbf{B}_s^{-1}\boldsymbol{\Gamma}_{\text{osc}} + \boldsymbol{\Gamma}_{\text{sea}} - \mathbf{B}\mathbf{B}_s^{-1}(\boldsymbol{\Gamma}_{\text{sea}} + \mathbf{D}_\theta \dot{\boldsymbol{\theta}}), \quad (7) \end{aligned}$$

where  $\boldsymbol{\Gamma}_{\text{osc}}$  is the torque command computed from the centralized-level WBOSC controller, which will be designed

in the next section; the torque feedback has a gain matrix  $\mathbf{I} - \mathbf{B}\mathbf{B}_s^{-1}$ , where the positive definite matrix  $\mathbf{B}_s$  is the desired motor inertia matrix [19]. From a physical interpretation, the torque feedback control is designed in the form of motor inertia shaping, which makes the passivity analysis tractable. Since we aim to reduce the effect of motor inertia on the joint-side dynamics, we choose  $\mathbf{B}_s \prec \mathbf{B}$ . As  $\mathbf{B}_s$  approaches zero (element-wise),  $\mathbf{I} - \mathbf{B}\mathbf{B}_s^{-1}$  becomes more negative, which implies larger torque feedback gains.

*Remark 1:* If the torque derivative term  $\mathbf{D}\mathbf{K}^{-1}\dot{\boldsymbol{\Gamma}}_{\text{sea}}$  is modeled on the left-hand side of Eq. (5), a corresponding torque derivative feedback term can be added in Eq. (7).

Besides this torque feedback loop, Eq. (7) contains a motor damping feedback  $\mathbf{D}_\theta \dot{\boldsymbol{\theta}}$  replacing the centralized-level Cartesian damping feedback. Combining Eqs. (5) and (7), we have

$$\boldsymbol{\Gamma}_{\text{osc}} = \mathbf{B}_s \ddot{\boldsymbol{\theta}} + \boldsymbol{\Gamma}_{\text{sea}} + \mathbf{D}_\theta \dot{\boldsymbol{\theta}}, \quad (8)$$

As a result, the overall SEA-aware multi-body dynamics are represented by the Lagrangian dynamics in Section II-A and the embedded-level SEA controller in Section II-B. Plugging Eq. (8) into Eq. (4), we have

$$\begin{aligned} \mathbf{A}(\mathbf{q})\ddot{\mathbf{q}} + \mathbf{U}^T \mathbf{B}_s \ddot{\boldsymbol{\theta}} + \mathbf{U}^T \mathbf{D}_\theta \dot{\boldsymbol{\theta}} + \mathbf{N}(\mathbf{q}, \dot{\mathbf{q}}) \\ + \mathbf{J}_s^T \mathbf{F}_r = \mathbf{U}^T \boldsymbol{\Gamma}_{\text{osc}}. \quad (9) \end{aligned}$$

Compared with conventional rigid multi-body dynamics, the following new terms emerge: shaped motor inertia  $\mathbf{U}^T \mathbf{B}_s \ddot{\boldsymbol{\theta}}$  and embedded motor damping feedback  $\mathbf{U}^T \mathbf{D}_\theta \dot{\boldsymbol{\theta}}$ . The ignored friction compensation and torque derivative can also be modeled as necessary [23].

### III. CENTRALIZED-LEVEL WBOSC WITH TIME DELAYS

In this section, we design the centralized-level Whole-Body Operational Space controller (WBOSC) on the left side of the control diagram in Fig. 1. The WBOSC with dynamically consistent contact constraints [1], [2] is expressed as

$$\boldsymbol{\Lambda}_{t|s} \ddot{\mathbf{x}} + \boldsymbol{\mu}_{t|s} + \mathbf{p}_{t|s} + \mathbf{F}_c = \bar{\mathbf{J}}_{t|s}^T (\mathbf{U}\mathbf{N}_s)^T \boldsymbol{\Gamma}_{\text{osc}}, \quad (10)$$

where  $\boldsymbol{\Lambda}_{t|s}$  is the task space inertia matrix under contact constraints;  $\boldsymbol{\mu}_{t|s}$  represents the centrifugal and Coriolis force;  $\mathbf{p}_{t|s}$  denotes the gravitational force;  $\mathbf{F}_c \in \mathbb{R}^6$  is a reaction force acting on the task point;  $\mathbf{J}^* = \mathbf{J}_{t|s} \bar{\mathbf{U}} \bar{\mathbf{N}}_s$  is the support consistent reduced Jacobian. The subscript  $t|s$  represents that the task is projected in the space consistent with *supporting constraints*. For more details, please refer to Def. 2.2.4 in [42].

Time delays intensely degrade the real-time control performance of humanoid robots [17]. Our previous work in [16] reveals that system stability and tracking performance is more sensitive to damping time delays rather than its stiffness counterpart. Thus Cartesian damping feedback is allocated to the embedded-level and represented by the motor damping feedback. In the WBOSC formalism, we denote the centralized-level round-trip time delay as  $T_H$  and the embedded-level round-trip time delay as  $T_L$ . These delays are time-varying and can be induced by communication

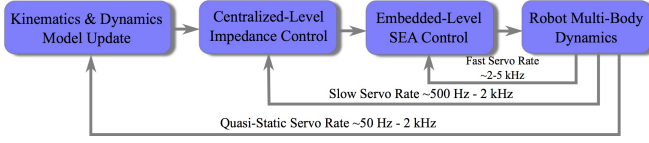


Fig. 2. A conceptual diagram for hierarchical control/dynamics layers with different servo rates. In certain cases, the kinematics and dynamics model uses the same update rate as that of the centralized-level controller [14].

channels, filtering, and computation. In general,  $T_H \gg T_L$  since  $T_H$  is usually dominated by large communication delays. For contact-free motion control (i.e.,  $F_c = 0$ ), the torque command  $\Gamma_{\text{osc}}$  computed at the centralized-level is

$$\begin{aligned} \Gamma_{\text{osc}}(t) &= \mathbf{J}^{*T}(t - \frac{T_H}{2}) \cdot \Lambda_{t|s}(t - \frac{T_H}{2}) \ddot{\mathbf{x}}(t) + \bar{\mathbf{g}}(\boldsymbol{\theta}(t - \frac{T_H}{2})) \\ &= \mathbf{J}^{*T}_{(-T_H/2)} \cdot \Lambda_{t|s,(-T_H/2)} \mathbf{K}_x (\mathbf{x}_d(t) - \mathbf{x}(t - \frac{T_H}{2})) \\ &\quad + \bar{\mathbf{g}}(\boldsymbol{\theta})_{(-T_H/2)}, \end{aligned} \quad (11)$$

where  $\mu_{t|s}$  is ignored for simplicity. The subscript  $-T_H/2$  stands for the instant  $t - T_H/2$ . The linear acceleration  $\ddot{\mathbf{x}}(t)$  is defined as

$$\ddot{\mathbf{x}}(t) = \mathbf{K}_x (\mathbf{x}_d(t) - \mathbf{x}(t - \frac{T_H}{2})). \quad (12)$$

Combining Eqs. (11) and (8),  $\Gamma_{\text{sea}}(t)$  can be derived as

$$\begin{aligned} \Gamma_{\text{sea}}(t) &= \Gamma_{\text{osc}}(t - \frac{T_H + T_L}{2}) - \mathbf{B}_s \ddot{\boldsymbol{\theta}}(t) - \mathbf{D}_\theta \dot{\boldsymbol{\theta}}(t) \quad (13) \\ &= \mathbf{J}^{*T}_{(-d_0)} \left( \Lambda_{t|s,(-d_0)} \mathbf{K}_x (\mathbf{x}_d(t - \frac{T_H + T_L}{2}) \right. \\ &\quad \left. - \mathbf{x}(t - T_H - \frac{T_L}{2})) \right) - \mathbf{B}_s \ddot{\boldsymbol{\theta}}(t) - \mathbf{D}_\theta \dot{\boldsymbol{\theta}}(t) \\ &\quad + \bar{\mathbf{g}}(\boldsymbol{\theta})_{(-d_0)}, \end{aligned} \quad (14)$$

where the matrices with subscript  $-d_0$  are evaluated at the instant  $t - d_0 = t - T_H - T_L/2$ .

As a brief summary, this WBSOC formulation is distinct from conventional Operational Space Control in terms of the following aspects: (i) Embedded-level SEA dynamics in Eq. (13) are modeled. (ii) The fast embedded damping feedback  $\mathbf{D}_\theta \dot{\boldsymbol{\theta}}$  takes the place of the slow centralized-level Cartesian velocity feedback. (iii) Distributed time delays are incorporated. Fig. 2 shows a diagram of nested control and dynamics layers with different servo rates.

#### IV. PASSIVITY OF TIME-DELAYED WBOSC

Given the time-delayed WBOSC formalism above, this section proposes a Lyapunov-Krasovskii functional (commonly used for the stability analysis of time-delay systems) to derive a passivity criterion for the overall closed-loop system. We subsequently generalize this passivity criterion to prioritized multi-task control.

##### A. Preliminaries

To guarantee the passivity condition, a majority of the existing literature derives the controller by only using motor angles  $\boldsymbol{\theta}$  and their derivative [40], [43]. In turn, the passivity

condition merely holds with respect to motor states. However, it is more physically meaningful to target joint-state-based passivity. In this study, we aim at this type of passivity by a one-to-one mapping  $\boldsymbol{\theta}_0 = \mathbf{h}(\mathbf{q}_0)$  between equilibrium points  $\boldsymbol{\theta}_0$  and  $\mathbf{q}_0$  under certain relaxed assumptions [23]. The mapping is defined as

$$\boldsymbol{\theta}_0 = \mathbf{h}(\mathbf{q}_0) = \mathbf{q}_0 + \mathbf{K}^{-1} \mathbf{l}(\mathbf{q}_0), \quad (15)$$

with a function  $\mathbf{l}(\mathbf{q})$  relating to feedback control and gravity compensation

$$\mathbf{l}(\mathbf{q}) = \mathbf{J}^*(\mathbf{q})^T \Lambda(\mathbf{q}) \mathbf{K}_x \tilde{\mathbf{x}}(\mathbf{q}) + \mathbf{g}(\mathbf{q}), \quad (16)$$

where the Cartesian position error is  $\tilde{\mathbf{x}}(\mathbf{q}_0) = \mathbf{x}_d(\mathbf{q}_0) - \mathbf{x}(\mathbf{q}_0)$ ;  $\mathbf{l}(\mathbf{q}) = \mathbf{l}(\mathbf{q})|_{\mathbf{q}=\mathbf{q}_0} = \mathbf{K}(\boldsymbol{\theta}_0 - \mathbf{q}_0)$ . Let us define a new state variable  $\bar{\mathbf{q}}$ , as a function of the motor angle  $\boldsymbol{\theta}$  only, that is equal to the joint angle  $\mathbf{q}$  at static state. Indeed,  $\bar{\mathbf{q}}$  can not be solved from  $\boldsymbol{\theta}$  analytically by Eq. (15). Thus, we adopt an iterative computational method [23] to compute  $\bar{\mathbf{q}}$ . More details of this method are provided in the contraction mapping principle of the supplementary material<sup>1</sup>. As a result, the static joint state is expressed as  $\bar{\mathbf{q}}(\boldsymbol{\theta}) = \mathbf{h}^{-1}(\boldsymbol{\theta})$ . The merit of using variable  $\bar{\mathbf{q}}$  rather than  $\mathbf{q}$  or  $\boldsymbol{\theta}$  is to make the passivity analysis tractable since a coupling between motor and joint positions is canceled. Meanwhile, the joint-side Cartesian stiffness is maintained.

Given the state  $\bar{\mathbf{q}}$  defined above, the centralized-level WBOSC in Eq. (11) is reformulated as

$$\begin{aligned} \Gamma_{\text{osc}}(t) &= \mathbf{J}^*(\bar{\mathbf{q}})^T_{(-T_H/2)} \Lambda(\bar{\mathbf{q}})_{(-T_H/2)} \mathbf{K}_x \left( \mathbf{x}_d(\bar{\mathbf{q}}(t)) \right. \\ &\quad \left. - \mathbf{x}(\bar{\mathbf{q}}(t - \frac{T_H}{2})) \right) + \bar{\mathbf{g}}(\boldsymbol{\theta})_{(-T_H/2)}, \end{aligned} \quad (17)$$

where  $\bar{\mathbf{q}}(t) = \bar{\mathbf{q}}(\boldsymbol{\theta}(t))$ ,  $\bar{\mathbf{q}}_0 = \bar{\mathbf{q}}(\boldsymbol{\theta}_0)$  at the static equilibrium.  $\dot{\mathbf{x}}(\bar{\mathbf{q}}) = \mathbf{J}^*(\bar{\mathbf{q}}) \dot{\bar{\mathbf{q}}}(t)$ . The subscript  $t|s$  is omitted for clarity.

*Remark 2:* The objective of gravity compensation is to find a  $\bar{\mathbf{q}}$  such that  $\mathbf{g}(\bar{\mathbf{q}}) = \mathbf{g}(\mathbf{q}) = \bar{\mathbf{g}}(\boldsymbol{\theta})$  in the quasi-static condition.  $\mathbf{g}(\bar{\mathbf{q}})$  corresponds to the gravitational force  $\mathbf{p}_{t|s}$  in the WBOSC of Eq. (10).

The overall time-delayed WBOSC is composed of Eqs. (4), (13) and (17), which will be used in the passivity analysis.

Another issue to take into account is the joint-angle-based Jacobian, where we have

$$\dot{\mathbf{x}}(\bar{\mathbf{q}}(\boldsymbol{\theta})) = \mathbf{J}^*(\bar{\mathbf{q}}) \dot{\bar{\mathbf{q}}}(\boldsymbol{\theta}) = \underbrace{\mathbf{J}^*(\bar{\mathbf{q}}) (\dot{\bar{\mathbf{q}}}(\boldsymbol{\theta}) - \dot{\boldsymbol{\theta}}(t))}_{\mathbf{v}_1} + \underbrace{\mathbf{J}^*(\bar{\mathbf{q}}) \dot{\boldsymbol{\theta}}(t)}_{\mathbf{v}_2}.$$

As will be shown in the proof, the passivity criterion requires a motor-angle-based Jacobian mapping, however. To this end, we adopt the energy tank method in [44] and introduce a new coordinate  $\hat{\mathbf{x}}(\bar{\mathbf{q}}(\boldsymbol{\theta}))$  defined as

$$\hat{\mathbf{x}}(\bar{\mathbf{q}}(\boldsymbol{\theta})) = \mathbf{u} + \mathbf{v}_2, \quad (18)$$

where  $\hat{\mathbf{x}}$  intends to track  $\dot{\mathbf{x}}$  while satisfying the passivity condition.  $\mathbf{u}$  is a velocity state deviating from  $\mathbf{v}_1$  to maintain

<sup>1</sup>Due to limited space, the supplementary material is provided in the following link [https://drive.google.com/open?id=0B\\_7VcYBOhr8uWHNybTRCbTJKenM](https://drive.google.com/open?id=0B_7VcYBOhr8uWHNybTRCbTJKenM)

the passivity. To compensate for the effect of  $\mathbf{u}$ , we define an energy storage function  $E_s$  as

$$E_s = \frac{1}{2}s^2, \quad (19)$$

which has the flow rate of change

$$\dot{s} = -\frac{1}{2s}\bar{d}_1\mathbf{u}^T\mathbf{Q}\mathbf{u} - \frac{1}{s}\bar{d}_1\mathbf{u}^T\mathbf{Q}\mathbf{v}_2. \quad (20)$$

We define the deviating term  $\mathbf{u}$  as

$$\mathbf{u} = \begin{cases} \mathbf{v}^{\text{ref}} & s > \epsilon \\ \mathbf{0} & \text{else} \end{cases} \quad (21a)$$

$$(21b)$$

with

$$\mathbf{v}^{\text{ref}} = \mathbf{v}_1 + \mathbf{K}_b(\mathbf{x}(\bar{\mathbf{q}}(\theta)) - \hat{\mathbf{x}}(\bar{\mathbf{q}}(\theta))). \quad (22)$$

If  $s > \epsilon > 0$  (i.e., a non-empty energy tank),  $\mathbf{u}$  converges to  $\mathbf{v}_1$  by using the position feedback control  $\mathbf{K}_b(\mathbf{x}(\bar{\mathbf{q}}(\theta)) - \hat{\mathbf{x}}(\bar{\mathbf{q}}(\theta)))$ . Passivity and null space performance are simultaneously guaranteed in this case. If  $s \leq \epsilon$  (i.e., an empty energy tank),  $\mathbf{u} = \mathbf{0}$ , which indicates the deviation of  $\hat{\mathbf{x}}(\bar{\mathbf{q}}(\theta))$  from  $\mathbf{x}(\bar{\mathbf{q}}(\theta))$ . In this case, the null space control performance is compromised to guarantee the system passivity. Note that Eq. (21) is designed to avoid a zero division of  $1/s$  in Eq. (20). The parameter  $\epsilon$  should be chosen close enough to zero such that the energy tank will never be empty (i.e., without the sacrifice of null space control performance). More details of the energy tank design are provided in [44].

Necessary propositions for the passivity criterion are shown in the supplementary material. From now on, without explicit notations, we assume the matrices  $\mathbf{J}^*$ ,  $\mathbf{\Lambda}$  and  $\bar{\mathbf{g}}(\theta)$  represent the time-delayed ones evaluated at time  $t - d_0$  in Eq. (14) for the sake of clarity. Additionally, we propose an assumption for upper bounds of time delays.

*Assumption 4:* (Upper bounds of time delays) Since the round trip delays  $T_H$  and  $T_L$  are time-varying, we define the upper bounds of the following delays:  $d_1 = T_H + T_L/2 \leq \bar{d}_1$ ,  $d_2 = (T_H + T_L)/2 \leq \bar{d}_2$ , which will be used afterwards.

### B. Passivity of WBOSC

This subsection derives a delay-dependent passivity criterion for the WBOSC with SEA dynamics. Let us first construct a Lyapunov-Krasovskii functional of the concerned time-delayed system [26] with  $V = V_1 + V_2 + V_3 + V_4$

$$\begin{aligned} V_1 &= \frac{1}{2}\dot{\mathbf{q}}^T\mathbf{A}(\mathbf{q})\dot{\mathbf{q}} + \mathcal{P}_g(\mathbf{q}) + \int_0^t (\dot{\mathbf{q}}^T(\delta)\mathbf{J}_s^T\mathbf{F}_r(\delta))d\delta, \\ V_2 &= \frac{1}{2}\dot{\theta}^T\mathbf{B}_s\dot{\theta} + \frac{1}{2}(\theta - \mathbf{q}_j)^T\mathbf{K}(\theta - \mathbf{q}_j), \\ V_3 &= -V_l(\theta) = \frac{1}{2}\tilde{\mathbf{x}}(\bar{\mathbf{q}}(\theta))^T\mathbf{\Lambda}\mathbf{K}_x\tilde{\mathbf{x}}(\bar{\mathbf{q}}(\theta)) - \frac{1}{2}\mathbf{l}^T(\bar{\mathbf{q}}(\theta)) \\ &\quad \mathbf{K}^{-1}\mathbf{l}(\bar{\mathbf{q}}(\theta)) - \mathcal{P}_g(\bar{\mathbf{q}}), \\ V_4 &= \frac{1}{2}\int_{-\bar{d}_1}^0\int_{t+r}^t\dot{\mathbf{x}}^T(\xi)\mathbf{Q}\dot{\mathbf{x}}(\xi)d\xi dr + E_s, \end{aligned}$$

where  $\mathbf{Q} \succ 0$ .  $V_1$  is an energy function corresponding to the multi-body dynamics in the joint-side subsystem of Fig. 3 while  $V_2$  corresponds to the SEA actuator dynamics

in the controller-side subsystem.  $V_3 = -V_l(\theta)$  represents a potential function for  $\mathbf{l}(\theta) = \mathbf{l}(\bar{\mathbf{q}}(\theta))$  of Eq. (16) and satisfies

$$\frac{\partial V_l(\theta)}{\partial \theta} = \bar{\mathbf{l}}(\theta)^T = \mathbf{l}(\bar{\mathbf{q}}(\theta))^T. \quad (23)$$

For more details about this potential function, please refer to (Appendix, [19]). The purpose of defining this potential function is to cancel certain terms in  $\dot{V}_2$  and  $\dot{V}_3$ , as will be illustrated later.  $V_4$  is a delay compensation term to be used together with Proposition 3 in the supplementary material.

Let us first prove the passivity of the joint-side subsystem via  $V_1$ . By the following properties

$$\frac{\partial \mathcal{P}_g(\mathbf{q})}{\partial \mathbf{q}} = \mathbf{g}(\mathbf{q}), \quad \frac{\partial \mathcal{P}_g(\bar{\mathbf{q}})}{\partial \bar{\mathbf{q}}} = \mathbf{g}(\bar{\mathbf{q}}), \quad (24)$$

and Eq. (4) and Property 2, the derivative of  $V_1$  is

$$\dot{V}_1 = \dot{\mathbf{q}}^T\mathbf{U}^T\mathbf{\Gamma}_{\text{sea}}. \quad (25)$$

Choosing the storage function of the joint-side subsystem in Fig. 3 as  $S_j(\mathbf{q}, \dot{\mathbf{q}}) = V_1$ , we have

$$\dot{S}_j(\mathbf{q}, \dot{\mathbf{q}}) = \dot{V}_1 = \dot{\mathbf{q}}^T\mathbf{U}^T\mathbf{\Gamma}_{\text{sea}} = \dot{\mathbf{q}}_j^T\mathbf{\Gamma}_{\text{sea}}. \quad (26)$$

Thus, the passivity of the mapping  $\mathbf{\Gamma}_{\text{sea}} \rightarrow \dot{\mathbf{q}}$  of Fig. 3 is guaranteed due to the inherent passive property of the physical system. Next, we prove the passivity of the controller-side subsystem in Fig. 3. Given a few mathematical manipulations in the supplementary material, the derivative of  $V_2$  is

$$\begin{aligned} \dot{V}_2 &= -\dot{\theta}^T\mathbf{D}_\theta\dot{\theta} - \dot{\mathbf{q}}_j^T\mathbf{\Gamma}_{\text{sea}} + \dot{\theta}^T\mathbf{J}^{*T}\mathbf{\Lambda}\mathbf{K}_x\int_{t-d_1}^t\dot{\mathbf{x}}(\xi)d\xi \\ &\quad + \dot{\theta}^T\mathbf{J}^{*T}\mathbf{\Lambda}\mathbf{K}_x(\hat{\mathbf{x}}_d - \hat{\mathbf{x}}) + \dot{\theta}^T\bar{\mathbf{g}}(\theta). \end{aligned} \quad (27)$$

As for  $\dot{V}_3$  and  $\dot{V}_4$ , we have

$$\begin{aligned} \dot{V}_3 &= -\frac{\partial \dot{V}_l(\theta)}{\partial \theta}\dot{\theta} = -\mathbf{l}^T(\bar{\mathbf{q}}(\theta))\dot{\theta} \\ &= -\dot{\theta}^T(\mathbf{J}^{*T}\mathbf{\Lambda}\mathbf{K}_x\tilde{\mathbf{x}}(\bar{\mathbf{q}}(\theta)) + \mathbf{g}(\bar{\mathbf{q}})), \\ \dot{V}_4 &= \frac{1}{2}\bar{d}_1\dot{\mathbf{x}}^T\mathbf{Q}\dot{\mathbf{x}} - \frac{1}{2}\int_{t-d_1}^t\dot{\mathbf{x}}(\xi)^T\mathbf{Q}\dot{\mathbf{x}}(\xi)d\xi + s\dot{s}. \end{aligned}$$

Without explicit notations, we define  $\hat{\mathbf{x}}(\bar{\mathbf{q}}(\theta)) = \hat{\mathbf{x}}(t) = \hat{\mathbf{x}}$ ,  $\hat{\mathbf{x}}_d = \hat{\mathbf{x}}_d(t)$ . For the components in  $\dot{V}_4$ , we have

$$\begin{aligned} \frac{1}{2}\bar{d}_1\dot{\mathbf{x}}^T\mathbf{Q}\dot{\mathbf{x}} + s\dot{s} &= \frac{1}{2}\bar{d}_1(\mathbf{u} + \mathbf{v}_2)^T\mathbf{Q}(\mathbf{u} + \mathbf{v}_2) \\ &\quad - \frac{1}{2}\bar{d}_1\mathbf{u}^T\mathbf{Q}\mathbf{u} - \bar{d}_1\mathbf{u}^T\mathbf{Q}\mathbf{v}_2 \\ &= \frac{1}{2}\bar{d}_1\mathbf{v}_2^T\mathbf{Q}\mathbf{v}_2 \\ &= \frac{1}{2}\bar{d}_1\dot{\theta}^T(t)\mathbf{J}^{*T}(\bar{\mathbf{q}})\mathbf{Q}\mathbf{J}^*(\bar{\mathbf{q}})\dot{\theta}(t), \end{aligned}$$

which is a favorable quadratic term of  $\dot{\theta}(t)$ . Additionally, by Property 3 in the supplementary material, we have

$$\begin{aligned} \dot{\theta}^T\mathbf{J}^{*T}\mathbf{\Lambda}\mathbf{K}_x\int_{t-d_1}^t\dot{\mathbf{x}}(\xi)d\xi - \frac{1}{2}\int_{t-d_1}^t\dot{\mathbf{x}}(\xi)^T\mathbf{Q}\dot{\mathbf{x}}(\xi)d\xi \\ \leq \frac{1}{2}\bar{d}_1\dot{\theta}^T(t)\mathbf{P}\dot{\theta}(t), \end{aligned} \quad (28)$$

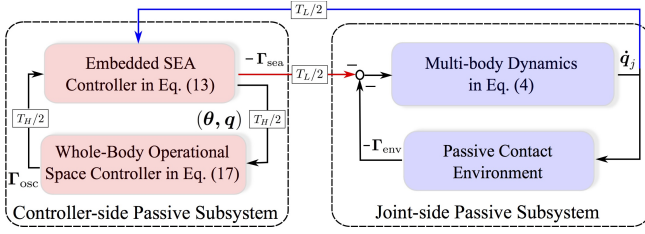


Fig. 3. Two passive subsystems interconnected in a feedback configuration. High- and low-level time delays  $T_H$  and  $T_L$  are labeled among subsystem blocks.

where  $\mathbf{P} = \mathbf{J}^{*T} \mathbf{\Lambda} \mathbf{K}_x \mathbf{Q}^{-1} \mathbf{K}_x \mathbf{\Lambda} \mathbf{J}^*$ . Since  $\mathbf{Q}^{-1} \succ 0$  and  $(\mathbf{J}^{*T} \mathbf{\Lambda} \mathbf{K}_x)^T = \mathbf{K}_x \mathbf{\Lambda} \mathbf{J}^*$ ,  $\mathbf{P}$  is positive definite. Let us define the storage function of the controller-side subsystem as  $S_c(\mathbf{q}, \boldsymbol{\theta}, \dot{\boldsymbol{\theta}}) = V_2 + V_3 + V_4$  and take its derivative

$$\begin{aligned} \dot{S}_c(\mathbf{q}, \boldsymbol{\theta}, \dot{\boldsymbol{\theta}}) &= \dot{V}_2 + \dot{V}_3 + \dot{V}_4 \leq -\dot{\boldsymbol{\theta}}^T \left( \mathbf{D}_\theta - \frac{1}{2} \bar{d}_1 \mathbf{P} \right. \\ &\quad \left. - \frac{1}{2} \bar{d}_1 \mathbf{J}^{*T}(\bar{\mathbf{q}}) \mathbf{Q} \mathbf{J}^*(\bar{\mathbf{q}}) \right) \dot{\boldsymbol{\theta}} - \dot{\mathbf{q}}_j^T \boldsymbol{\Gamma}_{\text{sea}}. \end{aligned}$$

If the first quadratic term is negative definite, the passivity of  $S_c(\mathbf{q}, \boldsymbol{\theta}, \dot{\boldsymbol{\theta}})$  is guaranteed. That is, the mapping  $\dot{\mathbf{q}} \rightarrow -\boldsymbol{\Gamma}_{\text{sea}}$  is passive in Fig. 3. Combining Eqs. (25)-(28), we have

$$\begin{aligned} \dot{V} &= \dot{V}_1 + \dot{V}_2 + \dot{V}_3 + \dot{V}_4 \leq \dot{\boldsymbol{\theta}}^T \left( -\mathbf{D}_\theta + \frac{1}{2} \bar{d}_1 \mathbf{P} \right. \\ &\quad \left. + \frac{1}{2} \bar{d}_1 \mathbf{J}^{*T}(\bar{\mathbf{q}}) \mathbf{Q} \mathbf{J}^*(\bar{\mathbf{q}}) \right) \dot{\boldsymbol{\theta}}. \end{aligned}$$

To guarantee  $\dot{V} \leq 0$ , we propose the following theorem.

**Theorem 1 (Passivity Criterion):** If there exists a positive-definite matrix  $\mathbf{Q}$  and a positive time delay scalar  $\bar{d}_1$  such that the following LMI holds:

$$\begin{pmatrix} -\mathbf{D}_\theta + \frac{1}{2} \bar{d}_1 \mathbf{J}^{*T}(\bar{\mathbf{q}}) \mathbf{Q} \mathbf{J}^*(\bar{\mathbf{q}}) & \frac{1}{2} \bar{d}_1 \mathbf{J}^{*T}(\bar{\mathbf{q}}) \mathbf{\Lambda} \mathbf{K}_x \\ * & -\frac{1}{2} \bar{d}_1 \mathbf{Q} \end{pmatrix} \preceq \mathbf{0}, \quad (29)$$

with  $*$  denoting the transpose of the corresponding matrix blocks, then the interconnected feedback system is passive and the motor velocity state  $\dot{\boldsymbol{\theta}}$  is bounded.

The delay-dependent criterion in Eq. (29) is derived by the Schur complement (see Proposition 5 in the supplementary material). Eq. (29) shows that as the motor damping feedback

$$\begin{pmatrix} -\mathbf{D}_\theta + \frac{1}{2} \bar{d}_1 \sum_{i=1}^N \mathbf{J}_{i|\text{prec}(i)}^{*T}(\bar{\mathbf{q}}) \mathbf{Q}_i \mathbf{J}_{i|\text{prec}(i)}^*(\bar{\mathbf{q}}) & \frac{1}{2} \bar{d}_1 \mathbf{M}_1 & \cdots & \frac{1}{2} \bar{d}_1 \mathbf{M}_N \\ * & -\frac{1}{2} \bar{d}_1 \mathbf{Q}_1 & \mathbf{0} & \mathbf{0} \\ * & * & \ddots & \mathbf{0} \\ * & * & * & -\frac{1}{2} \bar{d}_1 \mathbf{Q}_N \end{pmatrix} \preceq \mathbf{0}, \quad (31)$$

## V. SIMULATIONS

As a proof of concept, this section uses two simulations to (i) validate the proposed passivity criterion and (ii) test the torque control performance of WBOSC. The dynamic simulation adopts the recursive dynamics algorithm in [37] for the free floating multi-body dynamics of a point-foot bipedal robot with 3 DOF per leg. Model parameters are

gain matrix  $\mathbf{D}_\theta$  increases, larger time delays are allowable. We will validate this property in the simulation.

Note that, the matrices  $\mathbf{J}^*(\bar{\mathbf{q}})$  and  $\mathbf{\Lambda}$  in Eq. (29) are evaluated at time instant  $t - T_H - T_L/2$ . These matrices are treated as quasi-static ones given they are updated at a relatively slow servo rate. Therefore, we solve this LMI numerically. Compared to time-invariant LMI solutions, the feasible solution range of  $\mathbf{D}_\theta$  and  $\bar{d}_1$  in Eq. (29) becomes constrained. Given a fixed  $\mathbf{D}_\theta$ , the allowable maximum delay  $\bar{d}_1$  is solvable [30].

Based on the theorem above, we can generalize the passivity criterion to prioritized multi-task control as follows.

**Corollary 1 (Passivity of Prioritized Multi-task Control):**

Consider  $N$  prioritized Whole-Body Operational Space tasks. If there exists a set of positive-definite matrices  $\mathbf{Q}_i, i \in [1, N]$  and a positive time delay scalar  $\bar{d}_1$  such that the LMI in Eq. (31) holds, where  $\mathbf{M}_i = \mathbf{J}_{i|\text{prec}(i)}^{*T}(\bar{\mathbf{q}}) \mathbf{\Lambda}_{i|\text{prec}(i)} \mathbf{K}_{x,i}$ , then the interconnected feedback system is passive for this prioritized multi-task control and the motor velocity  $\dot{\boldsymbol{\theta}}$  is bounded.

*Proof:* Given the prioritized multi-task control structure in (Corollary 3.2.2, [42]), this proof is derived by following a procedure similar to that of Theorem 1. A few mathematical terms are augmented as below.

$$\hat{V}_4 = \frac{1}{2} \sum_i^N \int_{-\bar{d}_1}^0 \int_{t+r}^t \dot{\hat{\mathbf{x}}}_i^T(\xi) \mathbf{Q}_i \dot{\hat{\mathbf{x}}}_i(\xi) d\xi dr + E_s, \quad (30)$$

and a potential function  $\hat{l}(\mathbf{q})$  is

$$\hat{l}(\mathbf{q}) = \sum_i^N \mathbf{J}_{i|\text{prec}(i)}^{*T}(\mathbf{q}) \mathbf{\Lambda}_{i|\text{prec}(i)}(\mathbf{q}) \mathbf{K}_{x,i} \tilde{\mathbf{x}}_i(\mathbf{q}) + \mathbf{g}(\mathbf{q}),$$

then by following the same procedure, we have

$$\begin{aligned} \dot{V} &\leq \dot{\boldsymbol{\theta}}^T \left( -\mathbf{D}_\theta + \frac{1}{2} \bar{d}_1 \sum_i^N \mathbf{P}_i \right. \\ &\quad \left. + \frac{1}{2} \bar{d}_1 \sum_i^N \mathbf{J}_{i|\text{prec}(i)}^{*T}(\bar{\mathbf{q}}) \mathbf{Q}_i \mathbf{J}_{i|\text{prec}(i)}^*(\bar{\mathbf{q}}) \right) \dot{\boldsymbol{\theta}}, \end{aligned}$$

with  $\mathbf{P}_i = \mathbf{M}_i \mathbf{Q}_i^{-1} \mathbf{M}_i^T$ . Then the result in Eq. (31) follows. ■

consistent with our Hume bipedal robot [14]. The locomotion scenario is a 7-step bipedal walking process over rough terrain [45]. For the sake of simplicity, we only concern the dynamics of one leg. The operational space task is assigned as the 6-DOF center of mass positions and orientations.

In the first simulation, we solve the allowable maximum time delay via the LMI-based passivity criterion in Eq. (29).

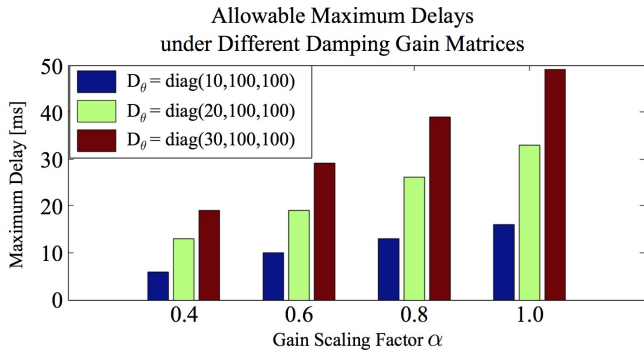


Fig. 4. Allowable maximum delays. The motor damping gain matrix we use is  $\alpha \cdot D_\theta$ , where  $\alpha$  is a scaling factor. Increasing  $\alpha$  enables a larger maximum delay  $\bar{d}_1$ . For each scaling factor  $\alpha$ , three tests are conducted by adjusting the first element of  $D_\theta$ , i.e., the hip abduction/adduction motor damping gain. As this damping gain increases, we can achieve a larger allowable maximum delay.

We specify *a priori* the nominal motor damping gain matrix  $D_\theta = \text{diag}\{10, 100, 100\}$  Nms/rad for one leg (i.e., hip abduction/adduction motor, hip flexion/extension motor, and knee flexion/extension motor) and the CoM Cartesian stiffness gain matrix  $K_x = \text{diag}\{100, 100, 100, 50, 50, 50\}$  N/m (Nm/rad) for CoM positions and orientations. We numerically evaluate the system matrices  $J^*(\bar{q})$  and  $\Lambda$  at each time instant of the entire locomotion process, and compute the maximum time delay which guarantees the feasibility of all LMIs associated with all these system matrices. A bisection algorithm is used together with the off-the-shelf Matlab LMI-optimization solver [46] to search the maximum delay solution. Fig. 4 shows the maximum delays under different damping feedback gain matrices. The result indicates that as the gains in the motor damping matrix  $D_\theta$  increase, the WBOSC can tolerate larger maximum delays without becoming unstable. This result is consistent with the passivity criterion of Eq. (29).

In the second simulation, we test rough terrain locomotion under time-varying delays. We choose the delays as  $T_H(t) = 20 + 10\sin(t)$  ms and  $T_L(t) = 3 + 2\sin(t)$  ms. Fig. 5 reveals that the SEA torque command  $\Gamma_{\text{sea}}$  has a phase lag to the WBOSC command  $\Gamma_{\text{osc}}$ , which is caused by the feedforward channel delay. For  $\Gamma_{\text{sea}}$  with different  $\beta$ , it is observed that  $\Gamma_{\text{sea}}$  with the bigger  $\beta$  (black line) experiences an inferior torque transparency (i.e., a larger deviation from  $\Gamma_{\text{osc}}$ ). This phenomenon is explainable below: a larger  $B_s$  leads to a smaller torque feedback gain  $I - BB_s^{-1}$ . Correspondingly, the actuator dynamics make a larger deviation of  $\Gamma_{\text{sea}}$  from  $\Gamma_{\text{osc}}$ . This conclusion can also be drawn from the torque relationship in Eq. (13). For more details about simulated robot parameters, please refer to the result in [14].

## VI. DISCUSSIONS AND CONCLUSIONS

In this study, we propose a class of time-delayed Whole-Body Operational Space Control (WBOSC) with series elastic actuator (SEA) dynamics. A novel Lyapunov-Krasovskii functional is designed to derive a delay-dependent LMI-based passivity criterion. This criterion is evaluated in a

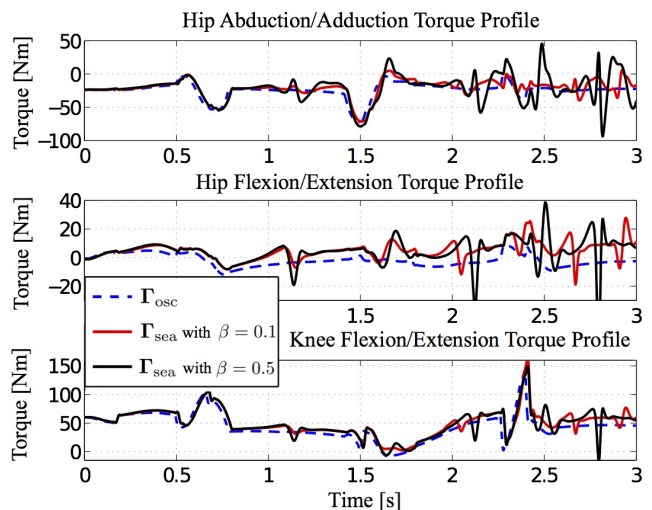


Fig. 5. WBOSC and SEA torque profiles under different shaped motor inertias. The shaped motor inertia matrix  $B_s = \beta \cdot B$ , where  $B = \text{diag}\{0.1357, 0.093, 0.093\}$  kg-m<sup>2</sup> is the diagonal physical motor inertia matrix of one 3-DOF Hume leg.  $\beta$  denotes a scaling factor.

dynamic locomotion simulation. This line of work lays the groundwork for achieving high performance SEA-aware WBOSC with time delays while guaranteeing the passivity.

Given the results of this study, the following conclusions for the passivity-based WBOSC are reached:

- The passivity criterion in Eq. (29) indicates that a larger stiffness gain matrix  $K_x$  is achievable given a larger motor damping gain matrix  $D_\theta$  or a smaller time delay  $\bar{d}_1$ . These parameter relationships are consistent with those in [22] established for virtual stiffness, virtual damping, and time delay.
- Increasing  $D_\theta$  enhances the WBOSC passivity as shown in Eq. (29), but deteriorates the SEA torque transparency as shown Eq. (13) (i.e.,  $\Gamma_{\text{sea}}$  has a larger deviation from  $\Gamma_{\text{osc}}$ ). This trade-off is analogous to the conflict of stability and transparency widely studied in the teleoperation community [27].
- The passivity criterion of the prioritized multi-task in Eq. (31) has a smaller solution range since finding multiple feasible  $Q_i, i \in [1, N]$  simultaneously poses more constraints. This conclusion meets our expectation.

A few promising problems that still need to be addressed in the future are summarized below: (i) Solve the time-varying system matrices of the passivity criteria in a more elegant way, such as the methods of solving time-varying LMIs online in [31] and convexifying matrices as a polytope of parametric matrices [32]; (ii) Model more practical round trip delays, such as asymmetric delays in feedforward and feedback channels. Literature from teleoperation and network communication fields [29], [30] will be instructive references; (iii) Design an optimal controller for the centralized-level WBOSC, and establish the mapping between the centralized-level and embedded-level damping gain matrices. [38] is a good reference; (iv) Conduct experimental validations on our legged robot [14]. It is meaningful to evaluate

the real performance affected by practical factors such as Coulomb friction and SEA torque bandwidth limit.

## REFERENCES

- [1] O. Khatib, "A unified approach for motion and force control of robot manipulators: The operational space formulation," *The International Journal of Robotics Research*, vol. 3, no. 1, pp. 43–53, 1987.
- [2] L. Sentis, J. Park, and O. Khatib, "Compliant control of multi-contact and center of mass behaviors in humanoid robots," *IEEE Transactions on Robotics*, vol. 26, no. 3, pp. 483–501, June 2010.
- [3] C. Ott, A. Dietrich, and A. Albu-Schäffer, "Prioritized multi-task compliance control of redundant manipulators," *Automatica*, vol. 53, pp. 416–423, 2015.
- [4] F. L. Moro, M. Gienger, A. Goswami, N. G. Tsarakis, and D. G. Caldwell, "An attractor-based whole-body motion control (wbmc) system for humanoid robots," in *IEEE-RAS International Conference on Humanoid Robots*, 2013, pp. 42–49.
- [5] N. Mansard, O. Khatib, and A. Kheddar, "A unified approach to integrate unilateral constraints in the stack of tasks," *IEEE Transactions on Robotics*, vol. 25, no. 3, pp. 670–685, 2009.
- [6] A. Dietrich, C. Ott, and A. Albu-Schäffer, "An overview of null space projections for redundant, torque-controlled robots," *The International Journal of Robotics Research*, 2015.
- [7] J. Nakanishi, R. Cory, M. Mistry, J. Peters, and S. Schaal, "Operational space control: A theoretical and empirical comparison," *The International Journal of Robotics Research*, vol. 27, no. 6, pp. 737–757, 2008.
- [8] A. Escande, N. Mansard, and P.-B. Wieber, "Hierarchical quadratic programming: Fast online humanoid-robot motion generation," *The International Journal of Robotics Research*, 2014.
- [9] S. Feng, E. Whitman, X. Xinjilefu, and C. G. Atkeson, "Optimization-based full body control for the darpa robotics challenge," *Journal of Field Robotics*, vol. 32, no. 2, pp. 293–312, 2015.
- [10] M. A. Hopkins, A. Leonessa, B. Y. Lattimer, and D. W. Hong, "Optimization-based whole-body control of a series elastic humanoid robot," *International Journal of Humanoid Robotics*, vol. 13, no. 01, 2016.
- [11] S. Kuindersma, R. Deits, M. Fallon, A. Valenzuela, H. Dai, F. Permenter, T. Koolen, P. Marion, and R. Tedrake, "Optimization-based locomotion planning, estimation, and control design for the atlas humanoid robot," *Autonomous Robots*, vol. 40, no. 3, pp. 429–455, 2016.
- [12] A. Herzog, N. Rotella, S. Mason, F. Grimmering, S. Schaal, and L. Righetti, "Momentum control with hierarchical inverse dynamics on a torque-controlled humanoid," *Autonomous Robots*, vol. 40, no. 3, pp. 473–491, 2016.
- [13] L. Saab, O. E. Ramos, F. Keith, N. Mansard, P. Soueres, and J.-Y. Fourquet, "Dynamic whole-body motion generation under rigid contacts and other unilateral constraints," *IEEE Transactions on Robotics*, vol. 29, no. 2, pp. 346–362, 2013.
- [14] D. Kim, Y. Zhao, G. Thomas, B. Fernandez, and L. Sentis, "Stabilizing series-elastic point-foot bipeds using whole-body operational space control," *IEEE Transactions on Robotics*, In Press, 2016.
- [15] H. Dai, A. Valenzuela, and R. Tedrake, "Whole-body motion planning with centroidal dynamics and full kinematics," in *IEEE-RAS International Conference on Humanoid Robots*, 2014, pp. 295–302.
- [16] Y. Zhao, N. Paine, K. S. Kim, and L. Sentis, "Stability and performance limits of latency-prone distributed feedback controllers," *IEEE Transactions on Industrial Electronics*, vol. 62, pp. 7151–7162, 2015.
- [17] C.-L. Fok, G. Johnson, L. Sentis, A. Mok, and J. D. Yamokoski, "ControlIt! a software framework for whole-body operational space control," *International Journal of Humanoid Robotics*, 2015.
- [18] N. Paine, J. S. Mehling, J. Holley, N. A. Radford, G. Johnson, C.-L. Fok, and L. Sentis, "Actuator control for the nasa-jsc valkyrie humanoid robot: A decoupled dynamics approach for torque control of series elastic robots," *Journal of Field Robotics*, vol. 32, no. 3, pp. 378–396, 2015.
- [19] C. Ott, A. Albu-Schäffer, A. Kugi, and G. Hirzinger, "On the passivity-based impedance control of flexible joint robots," *IEEE Transactions on Robotics*, vol. 24, no. 2, pp. 416–429, 2008.
- [20] A. Van der Schaft, *L2-gain and passivity techniques in nonlinear control*. Springer Science & Business Media, 2012.
- [21] J. E. Colgate and G. G. Schenkel, "Passivity of a class of sampled-data systems: Application to haptic interfaces," *Journal of robotic systems*, vol. 14, no. 1, pp. 37–47, 1997.
- [22] T. Hulin, A. Albu-Schäffer, and G. Hirzinger, "Passivity and stability boundaries for haptic systems with time delay," *IEEE Transactions on Control Systems Technology*, vol. 22, no. 4, pp. 1297–1309, 2014.
- [23] A. Albu-Schäffer, C. Ott, and G. Hirzinger, "A unified passivity-based control framework for position, torque and impedance control of flexible joint robots," *The International Journal of Robotics Research*, vol. 26, no. 1, pp. 23–39, 2007.
- [24] S.-H. Hyon, J. G. Hale, and G. Cheng, "Full-body compliant human-humanoid interaction: balancing in the presence of unknown external forces," *IEEE Transactions on Robotics*, vol. 23, pp. 884–898, 2007.
- [25] B. Henze, M. A. Roa, and C. Ott, "Passivity-based whole-body balancing for torque-controlled humanoid robots in multi-contact scenarios," *The International Journal of Robotics Research*, 2016.
- [26] K. Gu, J. Chen, and V. L. Kharitonov, *Stability of time-delay systems*. Springer, 2003.
- [27] D. A. Lawrence, "Stability and transparency in bilateral teleoperation," *IEEE Transactions on Robotics and Automation*, vol. 9, no. 5, pp. 624–637, 1993.
- [28] T. B. Sheridan, "Space teleoperation through time delay: review and prognosis," *IEEE Transactions on Robotics and Automation*, vol. 9, no. 5, pp. 592–606, 1993.
- [29] D. Lee and M. W. Spong, "Passive bilateral teleoperation with constant time delay," *IEEE Transactions on Robotics*, vol. 22, no. 2, pp. 269–281, 2006.
- [30] C.-C. Hua and X. P. Liu, "Delay-dependent stability criteria of teleoperation systems with asymmetric time-varying delays," *IEEE Transactions on Robotics*, vol. 26, no. 5, pp. 925–932, 2010.
- [31] D. Guo and Y. Zhang, "Zhang neural network for online solution of time-varying linear matrix inequality aided with an equality conversion," *IEEE Transactions on Neural Networks and Learning Systems*, vol. 25, no. 2, pp. 370–382, 2014.
- [32] P. Gahinet, P. Apkarian, and M. Chilali, "Affine parameter-dependent lyapunov functions and real parametric uncertainty," *IEEE Transactions on Automatic control*, vol. 41, no. 3, pp. 436–442, 1996.
- [33] G. A. Pratt, P. Willisson, C. Bolton, and A. Hofman, "Late motor processing in low-impedance robots: Impedance control of series-elastic actuators," in *American Control Conference*, vol. 4, 2004, pp. 3245–3251.
- [34] H. Vallery, J. Veneman, E. Van Asseldonk, R. Ekkelenkamp, M. Buss, and H. Van Der Kooij, "Compliant actuation of rehabilitation robots," *IEEE Robotics & Automation Magazine*, vol. 15, no. 3, pp. 60–69, 2008.
- [35] Y. Zhao, N. Paine, and L. Sentis, "Feedback parameter selection for impedance control of series elastic actuators," in *IEEE-RAS International Conference on Humanoid Robots*, 2014, pp. 999–1006.
- [36] R. Featherstone, *Rigid body dynamics algorithms*. Springer, 2014.
- [37] K.-S. Chang, "Efficient algorithms for articulated branching mechanisms: dynamic modeling, control, and simulation," Ph.D. dissertation, Stanford, 2000.
- [38] D. J. Braun, F. Petit, F. Huber, S. Haddadin, P. Van Der Smagt, A. Albu-Schäffer, and S. Vijayakumar, "Robots driven by compliant actuators: Optimal control under actuation constraints," *IEEE Transactions on Robotics*, vol. 29, no. 5, pp. 1085–1101, 2013.
- [39] M. W. Spong, "Modeling and control of elastic joint robots," *Journal of dynamic systems, measurement, and control*, vol. 109, no. 4, pp. 310–318, 1987.
- [40] P. Tomei, "A simple pd controller for robots with elastic joints," *IEEE Transactions on Automatic Control*, no. 10, pp. 1208–1213, 1991.
- [41] M. W. Spong, S. Hutchinson, and M. Vidyasagar, *Robot modeling and control*. Wiley New York, 2006, vol. 3.
- [42] L. Sentis, "Synthesis and control of whole-body behaviors in humanoid systems," Ph.D. dissertation, Stanford University, 2007.
- [43] L. Zollo, B. Siciliano, A. De Luca, E. Guglielmelli, and P. Dario, "Compliance control for an anthropomorphic robot with elastic joints: Theory and experiments," *Journal of Dynamic Systems, Measurement, and Control*, vol. 127, no. 3, pp. 321–328, 2005.
- [44] A. Dietrich, C. Ott, and S. Stramigioli, "Passivation of projection-based null space compliance control via energy tanks," *IEEE Robotics and Automation Letters*, vol. 1, no. 1, pp. 184–191, 2016.
- [45] Y. Zhao, B. Fernandez, and L. Sentis, "Robust phase-space planning for agile legged locomotion over various terrain topologies," in *Proceedings of Robotics: Science and Systems*, Ann Arbor, Michigan, 2016.
- [46] S. P. Boyd, L. El Ghaoui, E. Feron, and V. Balakrishnan, *Linear matrix inequalities in system and control theory*. SIAM, 1994, vol. 15.